Indian Journal of Engineering & Materials Sciences
Vol. 29, December 2022, pp. 809-816
DOI: 10.56042/ijems.v29i6.70298

Effect of Formability Process Parameters in Dynamic Strain Ageing Region of Austenitic Stainless Steel

Anitha Lakshmi[a*], Srinivasa Rao Ch.[b], Piyush Singhal[c]

[a]Department of Mechanical Engineering, GRIET, Hyderabad 500 090 India,
[b]Department of Mechanical Engineering, Andhra University, Visakhapatnam 530 003 India,
[c]Department of Mechanical Engineering, GLA University, Mathura 281 406 India,

Received : 9 September 2022; Accepted: 17 October 2022

The consumption of Austenitic Stainless-Steel ASS 304 has been increasing recently in the outer body of Automobile applications. Sheet Metal Forming is one of the processes used to convert ASS 304 sheet into an end product. ASS 304 has good ductility with the rise in temperature up to 450^{o}C and later dynamic strain aging (DSA) in the temperature range 450-600^{o}C. Formability studies of ASS 304 in the DSA region and the effect of process parameters like anisotropy and strain rate are investigated in the present paper. Stretch forming Investigations have been carried out at a temperature of 500^{o}C in two quasi-static strain rate ranges 1x 10^{-4} s^{-1} and 1x 10^{-1} s^{-1} concerning three orientations parallel (R_0), diagonal (R_{45}) and Transverse(R_{90}) to Rolling Direction. The experiments were carried out at both the necking and fracture regions. Deformed specimens' major and minor strains are measured to plot Fracture Forming limit Diagrams, strain distribution, and limiting Dome height. Particular attention is given to the evaluation of strain rate and orientation of the sheet concerning rolling direction on formability.

Keywords: ASS 304, Dynamic Strain Ageing (DSA), Forming Limit Diagram (FLD), Limiting Dome Height (LDH), Strain rate, Strain Distribution

1 Introduction

Due to several desirable qualities such as good mechanical properties and corrosion/oxidation resistance, austenitic stainless steels are widely used in versatile applications. Within a range of temperatures, understanding the serrated yielding mechanisms and how they affect the mechanical behaviour of austenitic stainless steels is critical for researching and designing improved steels for tougher environments. Alomari[1] has investigated Serration kinds, models defining the formation of the serrated flow, temperature-strain rate regimes for the development of serration, current findings of serration behaviour in a range of austenitic steels, and the impact of dynamic strain ageing[2-5]. The dynamic strain ageing DSA or Portevin -Lechatelier effect (PLC) region is changing in flow stress around mean value for a certain region. The diffusivity of the solute atoms is too low below this temperature range for them to segregate and lock at the dislocations during deformation. Beyond this range, the solute atoms' diffusivity is rapid enough to keep up with the moving dislocation motion neither generating drag nor inhibiting motion[6-8]. Under the effect of their contact energy, both are said to move in phases. Serrated plastic flow, negative strain rate sensitivity, and variations in ultimate tensile, as well as strain hardening with increasing temperature, are all possible physical symptoms of DSA. Lee et al. applied varied strain rates of 10^{-4} s^{-1}– 5 × 10^{-3} $s^{-1}$to Fe-19Cr-13Ni-0.2C austenitic stainless steel at 450^{o}C -550^{o}C during high-temperature tensile testing[9-12]. The serrated flow associated with plastic instability observed in stress-strain curves is linked to DSA induced by the interplay between dislocations and pipe diffusion of substitutional Cr atoms, according to the findings[13]. Serafim et al. have investigated the effect of strain rate on the deformation behaviour of different stainless steels. The mechanical tests show that as the strain rate is reduced, the strength of the material increases slightly[14]. For all steel specimens evaluated at a strain rate of 10^{-6} s^{-1} and below, intense serrations present in the stress-strain curves, which are attributed to dynamic strain ageing. Liu, Wen-qi, and Jun-he Lian[15] studied Under uniaxial tensile loading and general

*Corresponding author
(E-mail:anitha.akkireddy@gmail.com)

stress states, the DP1000 steel exhibits a characteristic DSA effect within a specified range of temperature and plastic strain under quasistatic loading. DSA usually begins at 100°C and increases from 200°C to 300°C. When the temperature reaches 400°C, the effect disappears. DSA provides thermal hardening, or increased strength as temperature rises, as well as wavy strain hardening characteristics[16-18]. Blue brittleness with short post-necking elongation is observed at low DSA temperatures (100-200°C) in terms of ductility. Surprisingly, at a high DSA temperature (300°C), the improved ductility is complemented by increased strength. A new design rule for materials in specific applications can be obtained by engineering DSA effects[18-20]. Punch and tensile stretching methods are commonly used in the industry to test and anticipate real-world automotive forming processes, including parametric geometries and technologies. According to Hecker, the most often used test is the out-of-plane approach, which employs the punch stretching geometry. [21]Ghosh and Hecker biaxial studies for in-plane and out-of-plane deformations demonstrated that strain stages received from sheet bending result in increased sheet formability. As a result, bending strain gradients for sheet materials must be considered in the study used to derive an FLC[22]. The Nakazima test[23] includes a hemispherical punch[24] and a selection of blanks held between a die and a circular blank holder. The simplicity of the tools and blanks in this last test makes it simple to obtain all of the loading paths required to construct an FLC[25].

Particular attention of this paper includes the evaluation of the impact of strain rate and orientation on the formability behaviour of ASS 304 during Dynamic strain ageing under stretch forming experiments.

2 Materials and Methods

2.1 Alloy worked and its weight composition

The Alloy ASS 304 is used for the present Investigation. The sheet is in cold rolled condition, 1 mm in thickness is considered for experimentation. For tensile testing the specimens are wire cut according to ASTM standard E8 (sub size) (Fig. 1(a) using wire cut Electro discharge (CNC) machine for higher precision accuracy and good finishing. For stretch forming tests the Nakazima specimens are considered for experimentation. The specimens for both tensile and stretching are wire cut along three orientations parallel(R_0), perpendicular (R_{90}) and diagonal (R_{45}) to the Rolling direction of the sheet, represented in Fig. 1 (b)

2.2 Tensile Testing in DSA Region

Many Investigations show that ASS 304 underwent Dynamic strain aging in the temperature range 300°C to 600°C. In DSA Region a serrated flow in the flow curve can be observed. In the present work the tensile tests are conducted at 500°C (falls within DSA Region) with varying process parameters of strain rate ranging $0.1s^{-1}$ to $0.0001\ s^{-1}$ in three orientations wrt sheet rolling direction i.e. parallel (R_0), diagonal (R_{45}) and Transverse (R_{90}). A total of six experiments are conducted using experimental setup of maximum 5 Ton capacity Servo Electric Hot forming machine with attached split furnace (two zone) can be heated up to 1000°C as shown in Fig. 2. It consists of two puller rods and four washers made of High strength and temperature resistant Inconel Alloy to hold the specimen tightly without any gap.

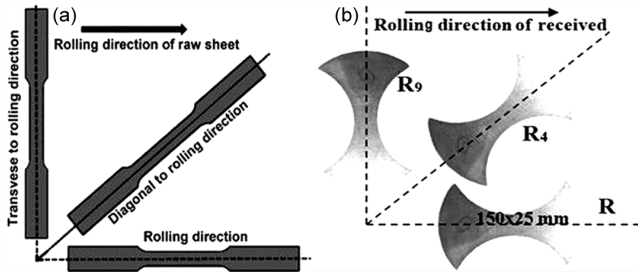

Fig. 1 — (a) Pictorial representation of specimens cut in three orientations, and (b) ASTM standard E8 (sub size) specimen

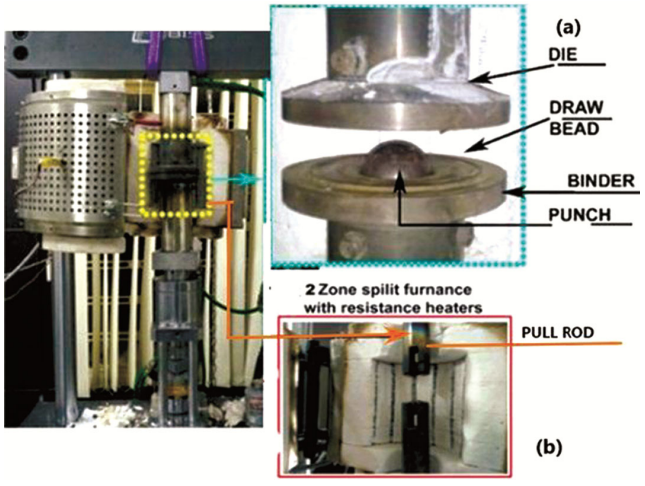

Fig. 2 — Stretch forming set up showing 2 Zone split furnace (a) $0.1s^{-1}$, and (b) $0.0001s^{-1}$

2.3 Mechanical Properties in DSA

The load displacement data from tensile tests is used to estimate engineering stress, strain, true stress, strain and material properties like yield strength, Young's modulus, Ultimate tensile strength, % elongation, strain hardening exponent and strength coefficient for 6 tensile specimens tested.

2.4 Stretch Forming in DSA Region

For stretch forming experimentation Nakazima specimens of dimensions 150x150, 150x125, 150x100, 150x75, 150x50,150x25 in mm a total of 12 blanks are considered for every case of process input parameter both in fracture as well necking region. Same tensile testing process parameters are repeated for stretch forming so that formability can be better predicted in multi axial loading compared to uniaxial loading. Six cases are carried out involving a total of 12x6 = 72 blanks. The same experimental test setup is used with attachments like punch, upper die, lower die, blank holding unit, punch encoder and load sensor to quantity force and displacement and data interface for acquisition of data. To measure the elongation the blank is etched chemically with circles of 2.5 mm diameter along with grid lines. Constant Blank holding force of 20 bar to prevent drawing of the sheet and Molycote lubricant to prevent oxidation are one of the inputs to the testing. The testing is done at elevated temperatures so laser etching is done instead of chemical etching to avoid erasing of chemically etched circles.

2.5 Plotting of experimental Forming Limit Diagram (FLD) in DSA

After experimental hemispherical dome punch testing of blanks, the etched circles gets deformed into ellipses as shown in Fig.3.These change in diameters are measured accurately using stereo zoom microscope. The average of three observations is taken as a measurement. The Minor and major strains in safe, necking and fracture are measured. The strains are scatter plotted on abscissa and ordinate in safe, necking and fracture region. A Safe Forming Limit curve (SFLC) is drawn between safe and necking strains. A Fracture Forming Limit (FFLD) curve is constructed differentiating between necking and fracture strains.

3 Results and Discussion

The ASS 304 is evaluated for variation in mechanical properties at two variables i.e. strain rate (0.1 s^{-1} (high), 0.0001 s^{-1}(low) and orientation (R_0, R_{45}, R_{90}) of sheet. From experimental tests as shown in Table 1. It was observed that there is much effect of strain rate compared to orientation of sheet on mechanical properties.

It is observed that the true stress – true strain curve plotted in Fig.4 shows the serrations formed in DSA region strain rate and orientation. In the inset, the serrations at higher strain rates are minor and % elongation is less and deviation of curve wrt orientation is more. At lower strain i.e $0.0001s^{-1}$ major serrations are observed with increase in % elongation very less variation within flow curves among three orientations. Inspite of DSA phenomenon at lower strain rate there is increase in percentage of elongation observed microstructural changes

Table 1 — Mechanical Properties variation at lower and higher strain rates in DSA region

S.NO	1	2
Temp in ^oC	500	500
strain rate s^{-1}	0.1	0.0001
Rolling direction	R_0, R_{45}, R_{90}	R_0, R_{45}, R_{90}
UTS in MPa	342.99±2	268.11±3
YS in MPa	202.95±6	110.73±4
ain hardening coefficient n	0.384±0.002	0.342±0.005
% elongation	27.28±3	42.32±2
K in MPa	886.79±4	848.98±1

Fig. 3 — Experimentally stretched cups of ASS 304 formed at 500˚C, in three rolling directions at strain rate a) $0.1s^{-1}$,and (b) $0.0001s^{-1}$.

improving ductility of the material at warm working temperature.

For plotting experimental FLD mostly used and easy Hecker's approach is implemented. In this method the minor and major strains are calculated from the measurement of displacement in two primary directions of circle (marked on the specimen before a mechanical test) is scatter plotted as abscissa and ordinate. A curve (SFLC)is constructed differentiating the safe strains from the necking strains and another curve (FFLC) differentiating necking strains from fracture strains is constructed on the same FLD. The FLDs accurateness is in range of ±4% of the Engineering strain measurements. The FLDs constructed at 500°C R_0, R_{45}, R_{90} at $0.1s^{-1}$ and $0.0001s^{-1}$ are shown in Fig. 5 and Fig. 6. The solid blue line indicates Fracture forming limit curve (FFLC) and red dotted line indicates Safe Forming limit curve (SFLC). At $0.1s^{-1}$ R_0, R_{45}, R_{90} orientation the maximum safe major strain is found to be n=0.34 ±0.02 and maximum fracture major strain ellipse is found at n=0.47±0.03. The effect of rolling direction has very minimal effect on FLD which is minimal. At $0.0001s^{-1}$ R_0, R_{45}, R_{90} orientation the maximum safe major strain is found to be n=0.46±0.01and maximum fracture major strain ellipse is found at n=0.61 ±0.01. The effect of rolling direction has very minimal effect on FLD which is minimal can be seen from Fig. 6. The effect of strain rate on FLD is considerable where variation of the maximum safe major strain is found to be n=0.12±0.01 and maximum fracture major strain ellipse is found at n=0.15±0.02 at 10^{-1} and 10^{-4} strain rates.

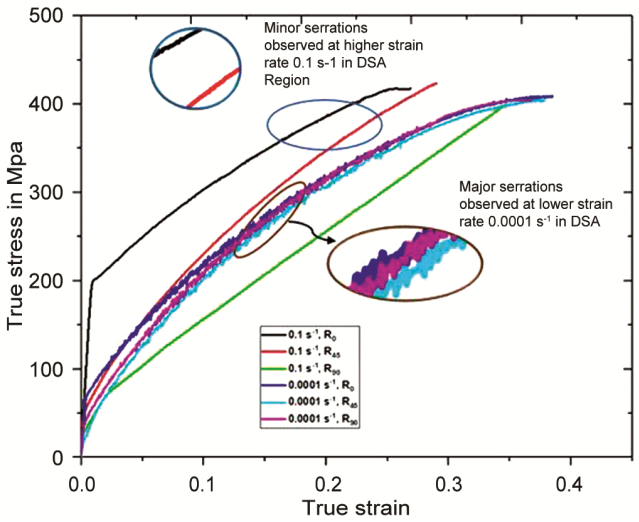

Fig. 4 — Variation in the serrations of flow curve w.r.t strain rates

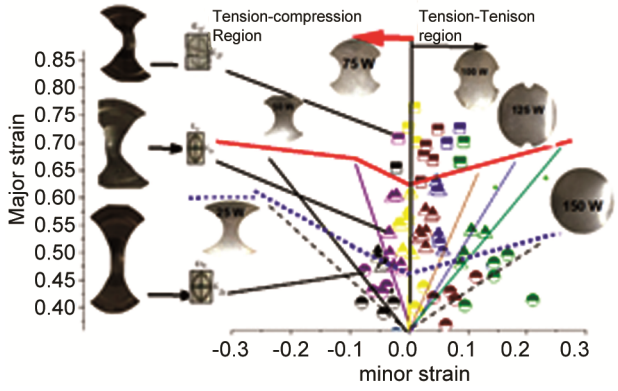

Fig. 5 — Experimental Forming limit diagram (FFLD) of 500°C, at $0.1s^{-1}$

The safe and fracture ellipses are more distributed in plane strain and tension-tension region compared to tension-compression region. With decrease in strain rate the slope of Forming limit curve is small in biaxial stretching region compared to 10^{-1} s^{-1} indicating the predominance role of major strains. It is observed from FLDs that at higher $0.1s^{-1}$ strain rate the band between the fracture and safe strains is less compared to the band gap at $0.0001s^{-1}$ (lower strain rates) in DSA Region.

To explain the formability of ASS 304 in DSA region, temperature and strain rate are considered as the most influencing parameters. To explain the formability in DSA Region temperature 500°C is taken as constant and parameter strain rate is varied in quasi static range in attempt to explain the extended formability. It is necessary to determine the formability limiting strains of any material before the forming operation. The limiting strains before necking are the safe limits for forming operation.

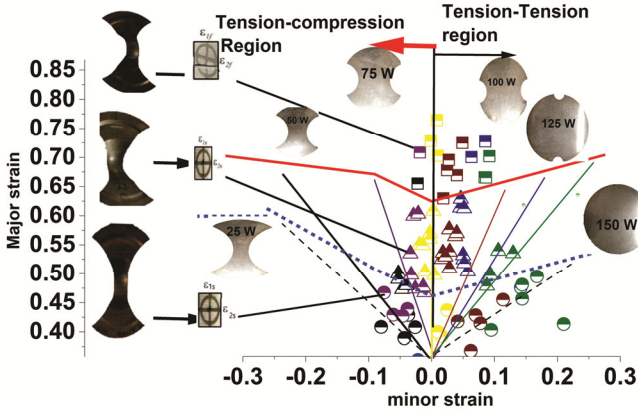

Fig. 6 — Experimental Forming Limit Diagram (FFLD) of 500°C, at $0.0001s^{-1}$.

With respect to strain rate i.e., at very low strain rate of $10^{-4}s^{-1}$ in DSA region represented in Fig. 7, the limiting strains are highest for samples cut parallel to the rolling direction $R_{0,}$ compared to the sheet sample cut transverse to the rolling direction. Whereas, at $10^{-1}s^{-1}$, the limiting strains are on higher side in R_{45} and R_{90} orientation wrt rolling direction in contrast to the sheet sample cut parallel to the rolling direction. The rolling direction samples of ASS 304 are indeed among the stronger samples investigated in this attempt, showing the effect of anisotropy. From the above statistics, it is also known that the gap between the curves decreases with a gradual increase in small strain wrt to Fig. 8, which indicates that the blank is safer at the lower minor strain level. It is known that nearly all the samples have better formability in all strain conditions, namely tension-compression, plain strain compression.

3.1. Limiting dome Height

The dome height of the stretched cups before fracture is measured using digital vernier height gauge at 500°C in three orientations $R_{0,}$ $R_{45,}$ R_{90} w.r.t to rolling direction at a range of The limiting dome height is considered as one of the important parameters for predicting formability at various varying input working conditions.

The difference in dome height of cups w.r.t variation in width of the specimen, orientations, strain rate at 500 ^{0}C temperature is shown in Fig. 9 (a-b). It is found from the Fig. 9 dome height is inversely related to the strain rate. The lower the strain rate the the more dome height of the cup. Forming of ASS 304 at 500^{0}C falls in DSA Region where strain hardening exponent is varying. It is noticed that there is variation in dome heights with increase in width of the blank up to plane strain region, whereas in tension-tension region from 125 mm width the dome height is directly proportional to increase in widths. At 500°C, $0.1s^{-1}$ blanks oriented at R_{45} showed better LDH =20.5 mm compared to R_0, R_{90} whereas at

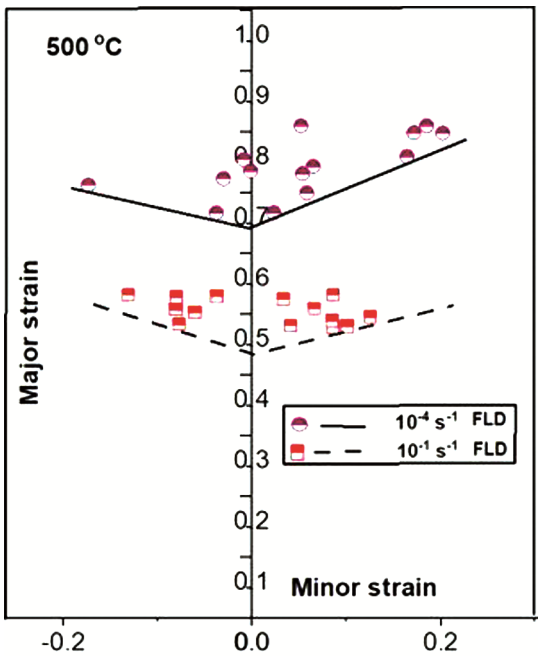

Fig. 8 — Enhanced FLD in two range of strain rates in DSA Region at 500°C

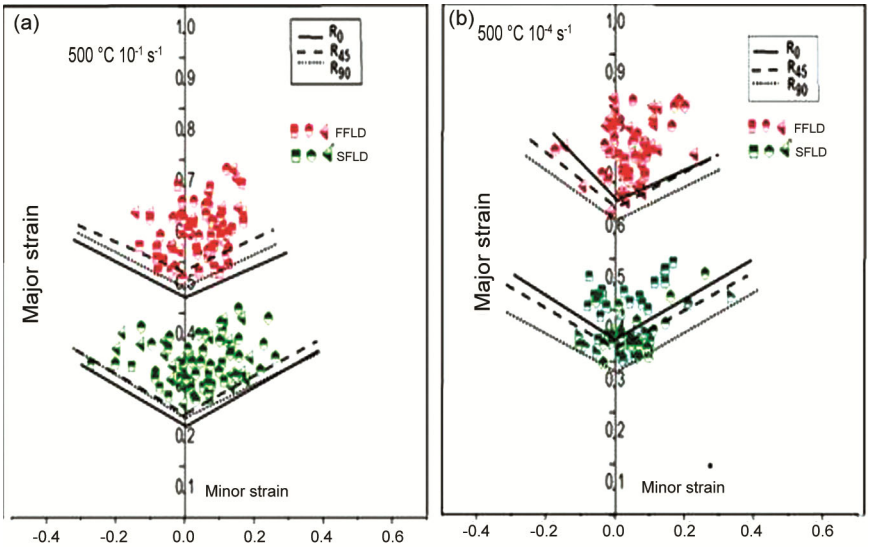

Fig. 7 — Comparison of Experimental FFLD and SFLD at 500^{0}C, in $R_{0,}$ $R_{45,}$ R_{90} at 9 (a)10^{-1} s^{-1} , and (b) 10^{-4} s^{-1}.

500°C, 0.0001s^{-1} blanks oriented at R_{90} showed better LDH =22.6 mm compared to R_0, R_{45}. In DSA region the formability of ASS 304 is improved at lower strain rates. Thus, with the right choice of strain rate the ASS 304 sheet in DSA can be formed without defects with minimum application of load as input.

3.2 Morphologies of Fractography

The fracture appearances of tensile specimens at 500°C wrt three orientations at strain rate 0.1 and 0.0001s^{-1}are photographed using scanning electron microscope. The mechanism for deformation at test temperature and phases present is analyzed through fractured micrographs. The best formability of ASS 304 at 500°C is found at 0.0001 s^{-1} lower strain rate and the micrograph at tested temperature showed failure at intergranular spaces indicating smooth grain surfaces as shown in and presence of new grain boundaries indicates crack propagation between new grains in DSA region at lower strain rates.

The variation of formability w.r.t orientations is considerably small and the fractography w.r.t orientations has not shown much variation in fracture appearances. At the same temperature and higher strain rates of 0.1 s^{-1} the formability strains are very low and the fracture appearance was intergranular with presence of more voids of less depth around inclusions of MnS which is predicted as responsible for brittle fracture. At higher strain rates there is less formability and the fracture mode is intergranular with the presence of shallow dimples denser in volume fraction as shown in Fig. 10(a). Whereas at lower strain rates the improvement in formability is due to presence coalescence of voids on fracture surface in shear deformed shoe shaped as shown in Fig. 10(b)

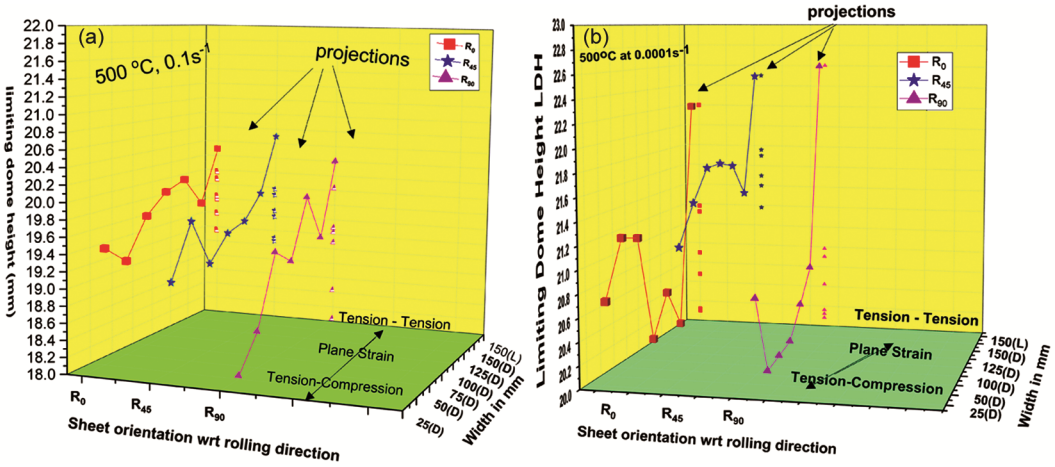

Fig. 9 — LDH of ASS 304 at 500°C, in three orientations R_0, R_{45}, R_{90} (a) 0.1s^{-1} (b) 0.0001s^{-1}

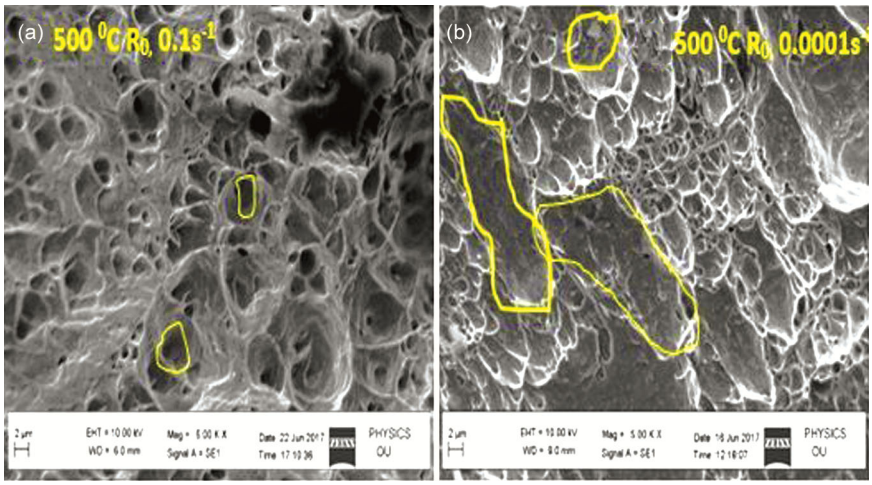

Fig. 10 — Micrographs showing variation in formation of voids on fracture surface wrt strain rate (a) 0.1 s^{-1} , and (b) 0.0001s^{-1}

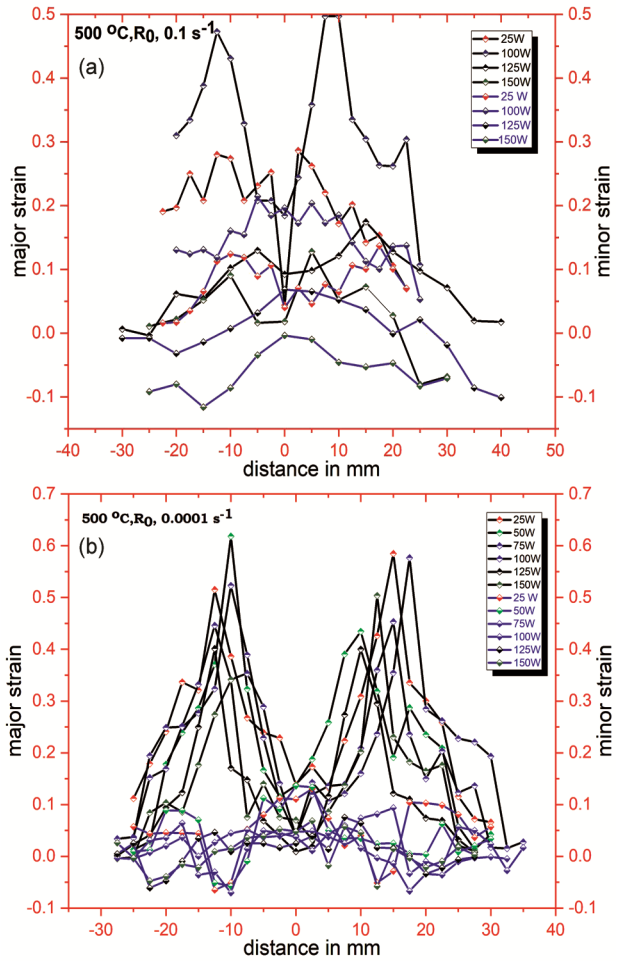

Fig. 11 — Strain distribution in cups stretched at (a) 500°C in three rolling directions, at 0.1 s-1 ,and (b) 0.0001 s-1 from different size blanks.

3.3 Strain Distribution

Stretching strain distribution patterns for all widths at 500°C temperature at 0.1 s^{-1} and 0.0001 s^{-1}strain rates represented in Fig. 11

For the whole blank width at 0.1 s^{-1} Figs 11 (a), there were two distinct peaks in significant strain, The symmetry in the size of strain maxima on either side of the pole could be owing to the fact that when the fracture started on one side of the pole, the load stopped acting on the other side, which was either in the safe or necked zone, and therefore the deformation stopped there. For the whole blank widths at 0.0001 s^{-1} from Figs. 11(b) and these peaks were symmetrically situated on either side of the pole (the centre of the ellipse that is lying exactly below the punch is referred to as pole and it is also the region which has undergone minimum amount of deformation).

4 Conclusion

- Isothermal deformation experiments are commonly used to investigate alloy flow behaviour. Warm forming operations are carried out on a servo electric hot forming test rig in order to analyze the impact formability process parameters of ASS 304 sheet in the DSA region at 500°C in the current study. The following conclusions can be taken from the experimental findings:
- During isothermal warm deformation, the limiting strains rose as the strain rate decreased, owing to the refinement of grain structures.
- The directionality of the sheet to the rolling direction is not well defined in these FLDs, since all of them melt into a single curve in the tension compression zone, showing the behaviour of planar isotropy in the material.
- The quality of hemispherical drawn cups is determined by measuring LDH and surface strains. The width of the sample and the experimental temperature are found to be directly proportional to LDH. Surface strain is shown to decrease first before increasing as the distance from the pole increases for both strain rates.
- The fracture is primarily ductile, according to SEM examination of the fractured component. The Fracture occurs through the thickness diagonally to the usual plane in all fractured specimens.
- In comparison to sheet orientation, the effect of strain rate has good formability behaviour on hot forming of ASS 304 sheets. Automobile industries require a formed component with excellent formability, hence this method is regarded as a challenging technique in the production design and development process.

Acknowledgement

The authors express their sincere gratitude toward the Gokaraju Rangaraju Institute of Engineering and Technology, Hyderabad for financially supporting the present work.

References

1 Alomari, & Abdullah S., *Materials at High Temperatures,* (2021) 1.
2 Lakshmi A, Buddi T, Subbiah R, & Bandhavi C, *E3S Web of Conf,* 184 (2020) 01036.
3 Lakshmi A A, Rao C S, Gangadhar J, Srinivasu C, & Singh S K, *Mat Today: Proc,* 4 2 (2017) 946.

4 Lakshmi A A, Rao C S, Srikanth M, Faisal K, Fayaz K, & Singh S K, *Mat Today: Proc,* 5 2 (2018) 3704.
5 Lakshmi A A, Ch Srinivasa Rao & Buddi T, *Mat Today: Proc,* 18 (2019) 2814.
6 Lakshmi A A, Rao C, Kotkunde N, Subbiah R, & Singh S K, *Int J Mech Eng Techno,l* 9 12 (2018) 403.
7 Reddy D M, Lakshmi A A & ul Haq. A., *Mat Today: Proc,* 19 (2019) 366.
8 Lakshmi A A, Rao C S, Gangadhar J, & Singh S K, *J of Adv in Technol and Eng Res,* 2 (2016) 52.
9 Serafim F M F, Oguocha I N A, Odeshi A G, Evitts R, Gerspacher R J, Ohaeri E G, & Alabi W O, *J Mat Eng Perfor,* 30 5 (2021) 3771.
10 Lakshmi A A, Ch S R, Sateesh N, & Subbiah R, *Adv Mat Process Technol,* (2021) 1.
11 Jayahari L, Sasidhar P V, Reddy P P, BaluNaik B, Gupta A K, & Singh S K, *J King Saud Uni-Eng Sci,* 26 1 (2014) 21.
12 Diepold B, Neumeier S, Meermeier A, Höppel H W, Sebald T, & Göken M, *Adv Eng Mat,* 23 10 (2021) 2001501.
13 Liu W & Jun-he L. *Intern J of Miner, Meta and Mat,* 28 (2021) 854.
14 Lade J, Singh S K, Banoth B N, & Gupta A K, *In AIP Conf Proc American Inst Phy,* 1567 1 (2013) 378.
15 Karthik V, Murugan S, Parameswaran P, Venkiteswaran C N, Gopal K A, Muralidharan N G, & Kasiviswanathan K V, *Energy Proc,* 7 (2011) 257.
16 Lee S Y, Takushima C, Hamada J I, & Nakada N, *Acta Materia,* 205 (2021) 116560.
17 Babu K A, Mandal S, Athreya C N, Shakthipriya B & Sarma V S, *Mater & Des,* 115 (2017) 262.
18 Bandyopadhyay K, Basak S, Prasad K S, Lee M G, Panda S K, & Lee J, *Intern J Solids and Struct,* 156 (2019) 263280.
19 Kotkunde N, Srinivasan S, Krishna G, Gupta A K, & Singh S K, *Trans of Nonferr Met Soc of China,* 26 3 (2016) 736.
20 Gupta A K, Singh S K, Reddy S, & Hariharan G, *Mat & Des,* 35 (2012) 589.
21 Hecker S S, *Sheet Met Ind,* 52 (1975) 671.
22 Ghosh A K, & Hecker S S, *Meta Trans,* 5 (1974) 2161.
23 Nakazima K, Kikuma T, Hasuka K, *Yawata Technol Rep,* 264 (1968) 8517.
24 Volk W, Groche P, Brosius A, Ghiotti A, Kinsey B L, Liewald M, Madej L, Min J, & Yanagimoto J, *CIRP Ann Manuf Technol,* 68 (2019) 775.